NUREG/CR-1241 Vol. I
HEDL-TME 80-4
R5

LWR PRESSURE VESSEL IRRADIATION SURVEILLANCE DOSIMETRY

QUARTERLY PROGRESS REPORT JANUARY - MARCH 1980

Hanford Engineering Development Laboratory

Operated by Westinghouse Hanford Company
P.O. Box 1970 Richland, WA 99352
A Subsidiary of Westinghouse Electric Corporation

Preparation coordinated by
G.L. Guthrie
W.N. McElroy

Manuscript Completed: August 1980
Date Published: December 1980

Prepared for Division of Reactor Safety Research
Office of Nuclear Regulatory Research
U.S. Nuclear Regulatory Commission
Washington, DC 20555
NRC FIN No. B5988-7

8101100857

NUREG/CR-1241 Vol. I
HEDL-TME 80-4

LWR PRESSURE VESSEL IRRADIATION SURVEILLANCE DOSIMETRY

QUARTERLY PROGRESS REPORT

January, February, March 1980

Preparation Coordinated by G. L. Guthrie, and W. N. McElroy
Hanford Engineering Development Laboratory

ABSTRACT

This report describes progress made in the Light Water Reactor Pressure Vessel Irradiation Surveillance Dosimetry Program during the reporting period.

The primary objective of the multi-laboratory program is to prepare an updated and improved set of dosimetry, damage correlation, and associated reator analysis ASTM Standards for LWR-PV irradiation surveillance programs. Supporting this objective are a series of analytical and experimental validation and calibration studies in "Standard, Referenc, and Controlled Environment Benchmark Fields", reactor "Test Regions", and operating power reactor "Surveillance Positions".

ACKNOWLEDGMENTS

The following organizations are presently participating in the Light Water Reactor Pressure Vessel Irradiation Surveillance Dosimetry Program and will periodically contribute to this report.

Atomic Energy Research Establishment, Harwell, England (AERE-H)

California State University Northridge (CSU-N)

Centre d'Etude de l'Energie Nucleaire - Studiecentrum Voor Kern Energie (CEN/SCK), Mol, Belgium

Electric Power Research Institute (EPRI)

Fracture Control Corporation (FCC)

General Electric Vallecitos Nuclear Center (GE-VNC)

Hanford Engineering Development Laboratory (HEDL)

IRT Corporation (IRT)

Kernforschungsanlage Julich Gmbh, Germany (KFA)

Macalester College (MC)

National Bureau of Standards (NBS)

Oak Ridge National Laboratory (ORNL)

Pacific Northwest Laboratories (PNL)

Radiation Research Associates (RRA)

Rockwell International Energy Systems Group (RIES)

Rolls-Royce and Associates Limited, Derby, England (RRAL)

Science Applications Incorporated (SAI)

University of California, Santa Barbara (UCSB)

University of Tennessee (UT)

Westinghouse Electric Corporation - PWR Systems Division (WEC-PWR-SD)

Westinghouse Electric Corporation - Research Division (WEC-RD)

FOREWORD

The light water reactor pressure vessel (LWR-PV) surveillance dosimetry program has been established by NRC in recognition of the importance of improving, maintaining, and standardizing neutron dosimetry, damage correlation, and the associated reactor analysis procedures used for predicting the integrated effect of neutron exposure to LWR pressure vessels. A vigorous research effort attacking the same measurement and analysis problems goes forward worldwide, and strong cooperative links between the NRC supported activities at HEDL, ORNL, and NBS and those supported by CEN/SCK (Mol, Belgium), EPRI (Palo Alto, USA), KFA (Jülich, Germany) and several U. K. laboratories have been established. The major benefit of this program will be a significant improvement in the accuracy of the assessment of the remaining safe operating lifetime of light water reactor pressure vessels.

The primary objective of the multilaboratory program is to prepare an updated and improved set of dosimetry, damage correlation, and associated reactor analysis ASTM Standards for LWR-PV irradiation surveillance programs. Supporting this objective are a series of analytical and experimental validation and calibration studies in "Standard, Reference, and Controlled Environment Benchmark Fields," reactor "Test Regions," and operating power reactor "Surveillance Positions."

These studies will establish and certify the precision and accuracy of the measurement and predictive methods which are recommended for use in the ASTM Standards. Consistent and accurate measurement and data analysis techniques and methods, therefore, will have been developed and validated along with guidelines for required neutron field calculations that are used to correlate changes in material properties with the characteristics of the neutron radiation field. It is expected that the application of the established ASTM Standards will permit the reporting of measured materials property changes and neutron exposures to an accuracy and precision within bounds of 10 to 30%, depending on the measured metallurgical variable and neutron environment.

The assessment of the radiation-induced degradation of masterial properties in a power reactor pressure vessel requires accurate definition of the neutron field from the outer region of the reactor core to the outer boundaries of the pressure vessel. Problems with measuring neutron flux and spectrum are associated with two distinct components of LWR-PV irradiation surveillance procedures: (1) proper application of calculational estimates of the neutron fluence delivered to in-vessel surveillance positions, various locations in the vessel wall, and ex-vessel support structures and surveillance positions, and (2) understanding the relationship between material property changes in reactor vessels, in vessel support structures, and in metallurgical test specimens in test reactors and at accelerated neutron flux positions in operating power reactors.

The first component requires validation and calibration experiments in a variety of neutron irradiation test facilities including LWR-PV mock-ups, power reactor surveillance positions, and related benchmark neutron fields. The benchmarks serve as a permanent measurement reference for neutron flux and fluence detection techniques, which are continually under development and widely applied by laboratories with different levels of capability. The second component requires a serious extrapolation of an observed neutron induced mechanical property change from test reactor "test regions" and operating power reactor "surveillance positions" to locations inside the body of the pressure vessel wall and ex-vessel support structures. The neutron flux at the vessel inner wall is up to one order of magnitude lower than at surveillance specimen positions and up to two orders of magnitude lower than for test reactor positions. At the vessel outer wall, the neutron flux is one order of magnitude or more lower than at the vessel inner wall. Further, the neutron spectrum at, within, and leaving the vessel is substantially altered.

In order to meet the reactor pressure vessel radiation monitoring requirements, a variety of neutron flux and fluence detectors are employed, most of which are passive. Each detector must be validated for application to the higher flux and harder neutron spectrum of the test reactor "test region"

and to the lower flux and degraded neutron spectrum at "surveillance positions". Required detectors must respond to neutrons of various energies so that multigroup spectra can be determined with accuracy sufficient for adequate damage response estimates. Proposed detectors for the program include radiometric detectors, helium accumulation fluence monitors, solid state track recorders, and damage monitors.

The necessity for pressure vessel mock-up facilities for dosimetry investigations and for irradiation of metallurgical specimens was recognized early in the formation of the NRC program. Experimental studies associated with high and low flux versions of a PWR pressure vessel mock-up are in progress. The low flux version is known as the Poolside Critical Assembly (PCA) and the high flux version is known as the Pool Side Facility (PSF). Both are located at ORNL. As specialized benchmarks, these facilities will provide well-characterized neutron environments where active and passive neutron dosimetry, various types of LWR-PV neutron field calculations, and temperature-controlled metallurgical damage exposures are brought together.

The results of the measurement and calculational strategies outlined here will be made available for use by the nuclear industry as ASTM Standards. Federal Regulation 10CFR50 already calls for adherence to several ASTM Standards which require establishment of a surveillance program for each power reactor and incorporation of flux monitors and post-irradiation neutron field evaluation. Revised and new standards in preparation will be carefully structured to be up-to-date, flexible, and, above all, consistent.

CONTENTS

FIGURES

TABLES

SUMMARY

HANFORD ENGINEERING DEVELOPMENT LABORATORY
(HEDL)

Thin foils of three separate steel alloys were irradiated at 150°C in a German reactor. Some of the irradiated foils were used as the subject of an earlier extensive German study of isochronal anneals relating hardness and annealing temperature for these steel alloys. A joint German-US program has been started to examine the foils with a transmission electron microscope. This program attempts to relate the appearance or disappearance of various structural features to changes in hardness after annealing the alloys at various temperatures. Prelimary examination reveals no difference between irradiated and unirradiated specimens prior to the initiation of the annealing treatments.

A large data bank was analyzed for statistical features that would indicate errors attributable to incorrect fluence determinations. The data bank relates irradiation induced Charpy shift, copper content, and fluence for pressure vessel steel Charpy surveillance specimens in light water power reactors. The characteristic feature indicative of fluence errors is that the magnitude of the errors should correlate with the magnitude of the reported Charpy shift. The analysis shows that removal of the fluence errors will make an important improvement in the data, but the fluence errors are not responsible for the major part of the scatter.

Oak Ridge National Laboratory
(ORNL)

Funds to continue the transport calculations have been delayed to FY-81.

All scheduled differential and integral measurements at the PCA for the Westinghouse-HEDL simulated capsule (the full-power perturbation experiment) has been completed at the PSF. Also, extensive testing of the surveillance capsule was conducted in a temporary position in the ORR pool.

The measurements in the fourth NRC-HSST dosimetry experiments were evaluated. Evaluation of the dosimetry in the PCA 8/7 and 12/13 configurations for comparison with calculated values in the PCA Blind Test were completed. Also, the results from the PCA calculational Blind Test were evaluated.

HANFORD ENGINEERING DEVELOPMENT LABORATORY (HEDL)

A. MICROSTRUCTURAL EXAMINATION OF NEUTRON-IRRADIATED PRESSURE VESSEL STEELS

L. E. Thomas

Objective

The purpose of this work is to determine the microscopic mechanisms associated with well-defined stages in the recovery of Vickers hardness and other mechanical properties during annealing of neutron-irradiated pressure vessel steels. The work is part of an investigation of the mechanisms responsible for saturation of irradiation embrittlement in these steels and was initiated by D. Pachur at the Nuclear Research Center, Julich, F.R.G.

Summary

Specimens of three pressure vessel steels irradiated to fluences from 1.5×10^{18} to 7×10^{19} n/cm^2, E>1 MeV, at 150°C in a German research reactor were received for an electron microscopy study of postirradiation annealing effects. This study focuses on the microstructural changes associated with various stages in the recovery of mechanical properties during annealing. The initial work concentrated on preparing transmission electron microscopy (TEM) specimens that were free from surface oxides and on characterizing microstructures of the as-received specimens.

Electron microscopic examination revealed no differences in dislocation structure or second-phase particles in irradiated and unirradiated specimens. Small defect clusters produced during irradiation were not detectable in the presence of surface oxide particles left by electropolishing. The as-received steels contained a mixture of 0.5 to 30 μm diameter grains with a recovered dislocation structure and many second-phase particles. Among these, two predominant phases were equally common. One, identified by electron diffraction as Fe_3C, has the characteristic metal composition Fe-11 wt. % Mn; the other contains 50 to 80 wt. % Mo with Fe and minor elements and is probably Mo_2C. Work on improving the electropolishing technique and specimen annealing is in progress.

Accomplishments and Status

1. Introduction

Irradiation embrittlement of ferritic steels used for LWR pressure vessels has been studied extensively for at least fifteen years. The embrittlement phenomenon is still not well understood, partly because the defects responsible may be too small even for TEM, but has been attributed to submicroscopic vacancy-copper atom aggregates.[1]

Commercial pressure vessel steels such as ASTM Type A533 Grade B manifest irradiation embrittlement by an increase in the ductile-brittle transition temperature (DBTT), a drop in the upper shelf energy in Charpy V-notch tests, and increases in yield strength and Vickers hardness. Pachur[2] finds that the recovery of these properties during four-hour isochronal annealing at 200°C to 500°C exhibits well-defined steps that apparently indicate the operation of four or five distinct recovery mechanisms. Figure HEDL-1 shows one of his annealing curves for Vickers hardness and the contribution of four processes which were determined from the time and temperature dependencies of the recovery. The contribution of individual processes to the overall recovery also depends on neutron fluence, as shown in Figure HEDL-2.

To investigate the microscopic mechanisms responsible for the observed recovery behavior, a cooperative program involving electron microscopic examination of Pachur's annealed specimens was initiated. Specimens of three steels, irradiated to fluences from 1.5×10^{18} to 7×10^{19} n/cm^2, E>1 MeV, were received at HEDL and prepared for annealing. Table HEDL-1 gives composition, irradiation conditions, properties, and recommended annealing temperatures for these specimens.

To date, work performed in the cooperative program has involved development of an electropolishing technique to prepare TEM specimens that are free of

POOR ORIGINAL

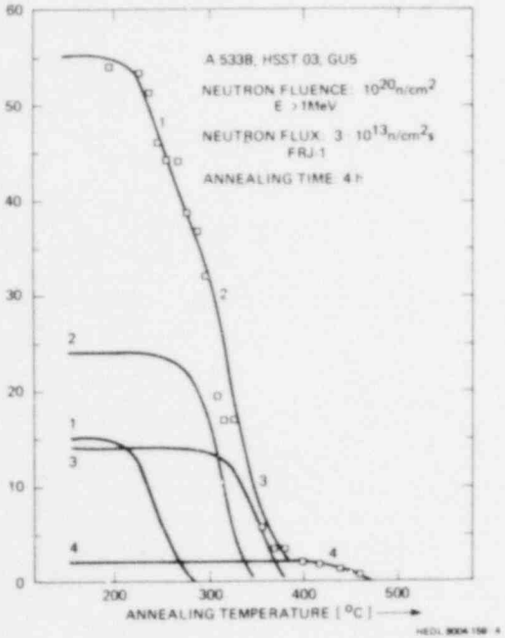

FIGURE HEDL-1. Recovery of Vickers Hardness in Neutron-Irradiated A533 B Steel During Four-Hour Isothermal annealing.

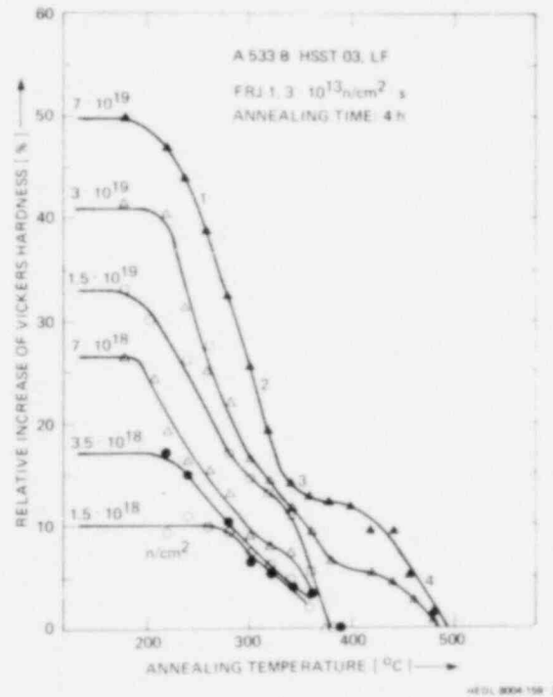

FIGURE HEDL-2. Recovery of Vickers Hardness in A533 B Steel Irradiated to Various Fluences during Four-Hour Isochronal Annealing. (from Reference 2)

TABLE HEDL-1
DATA FOR TEM SPECIMENS RECEIVED FROM D. PACHUR

Material	A 533 B HSST 03 LF					A 533 B Modified					Weld
Chemical Analysis wt %	0.22 C<0.0005 B 0.25 Si 0.01 Co 1.44 Mn 0.12 Cr 0.012 P 0.12 Cu 0.015 S 0.51 Mo 0.023 N 0.63 Ni 0.023 Al 0.01 V					0.11 C<0.001 B 0.35 Si 0.013 Co 1.36 Mn 0.11 Cr 0.012 P 0.11 Cr 0.008 S 0.37 Mo 0.016 N 1.5 Ni 0.014 Al 0.015 V					0.06 C<0.0003 B 0.21 Si 0.023 Co 1.85 Mn 0.08 Cr 0.012 P 0.29 Cu 0.003 S 0.56 Mo 0.011 N 1.3 Ni 0.015 Al 0.02 V
Capsule No.	KFA 1	KFA 2	KFA 3	KFA 4	KFA 5	KFA 6	KFA 7	KFA 8	KFA 9	KFA 10	KFA 11
Neutron Fluence n/cm^2 E>1 MeV	$1.5x10^{18}$	$1.5x10^{19}$	$1.5x10^{19}$	$3x10^{19}$	$7x10^{19}$	$1.5x10^{18}$	$1.5x10^{19}$	$1.5x10^{19}$	$3x10^{19}$	$7x10^{19}$	$5x10^{19}$
Neutron Flux FRJ-1 n/cm^2 E>1 MeV	$3x10^{13}$	$3x10^{13}$	$6x10^{11}$	$3x10^{13}$	$3x10^{13}$	$3x10^{13}$	$3x10^{13}$	$6x10^{11}$	$3x10^{13}$	$3x10^{13}$	$3x10^{13}$
Transition Temp. TT 30 Ft-Lb=51 J/cm^2	60°C	145°C	150°C	145°C	187°C	24°C	110°C	105°C	114°C	168°C	--
Increase of Transition Temp. TT	35°C	120°C	125°C	120°C	162°C	36°C	122°C	117°C	126°C	180°C	--
Vickers Hardness HV 10 N/mm^2	2200	2800	2700	2820	2980	2250	2800	2840	2930	3070	3440
Increase of Vickers Hardness	10%	40%	35%	41%	50%	23%	53%	55%	60%	68%	55%
Irradiation Temp.	150°C	150°C	150°C	150°C	150°C	150°C	150°C	150°C	150°C	150°C	150°C
Proposal for TEM Annealing Heat Treatment 1)	no	no	no	no	no	no	no	no	no	no	no
2)	330°C	260	280	260	270	310	270	290	270	270	290
3)	400	310	330	310	310	400	330	330	330	330	330
4)		400	400	400	400	490	400	400	400	400	400
5)		490	490	490	490		490	490	490	490	500
6)								600	600	600	

surface oxides, TEM microstructural characterization of as-received specimens, electron diffraction and energy-dispersive X-ray (EDX) microanalysis, and preparation of the specimens for annealing.

Experimental Methods and Procedures

1. Specimen Preparation

Surface oxide produced during specimen electropolishing presents a formidable problem in attempting TEM observation of small defect clusters in irradiation embrittled steels. It is possible to eliminate surface oxides and observe small radiation-induced defect clusters in Cu- and Au-doped iron alloys by subjecting A533 B steel specimens to jet electropolishing in an anhydrous sodium chromate/glacial acetic acid mixture (100 g in 500 ml) at about 22°C. The best results obtained, so far, were at 90 V, 120 mA, in a Metalthin electropolishing unit. However, even though freshly polished specimens appear oxide-free during TEM, selected area diffraction patterns taken near the foil edges show diffraction spots due to oxide on the specimen surfaces. Also, EDX analysis, performed with an ultrathin window EDX detector, directly confirmed the presence of considerable oxygen. Figure HEDL 3 shows an EDX spectrum taken from the A533 B steel. The carbon K X-ray peak in this spectrum is due to hydrocarbon contamination on the specimen. Clearly, further work is needed to produce oxide-free TEM specimens.

2. Analytical Microscopy

The energy-dispersive X-ray analyzer used in this work consists of a Kevex Model 6 UTW detector and Tracor-Northern 2000 multichannel analyzer, and operates on a JEOL Model 100CX (100 kV) analytical transmission/scanning transmission electron microscope. The computer-based analyzer employs commercially available software that deconvolutes overlapping X-ray spectra and provides quantitative elemental analyses. In the present work, the analyzer was used to check the overall alloy composition and to find the

POOR ORIGINAL

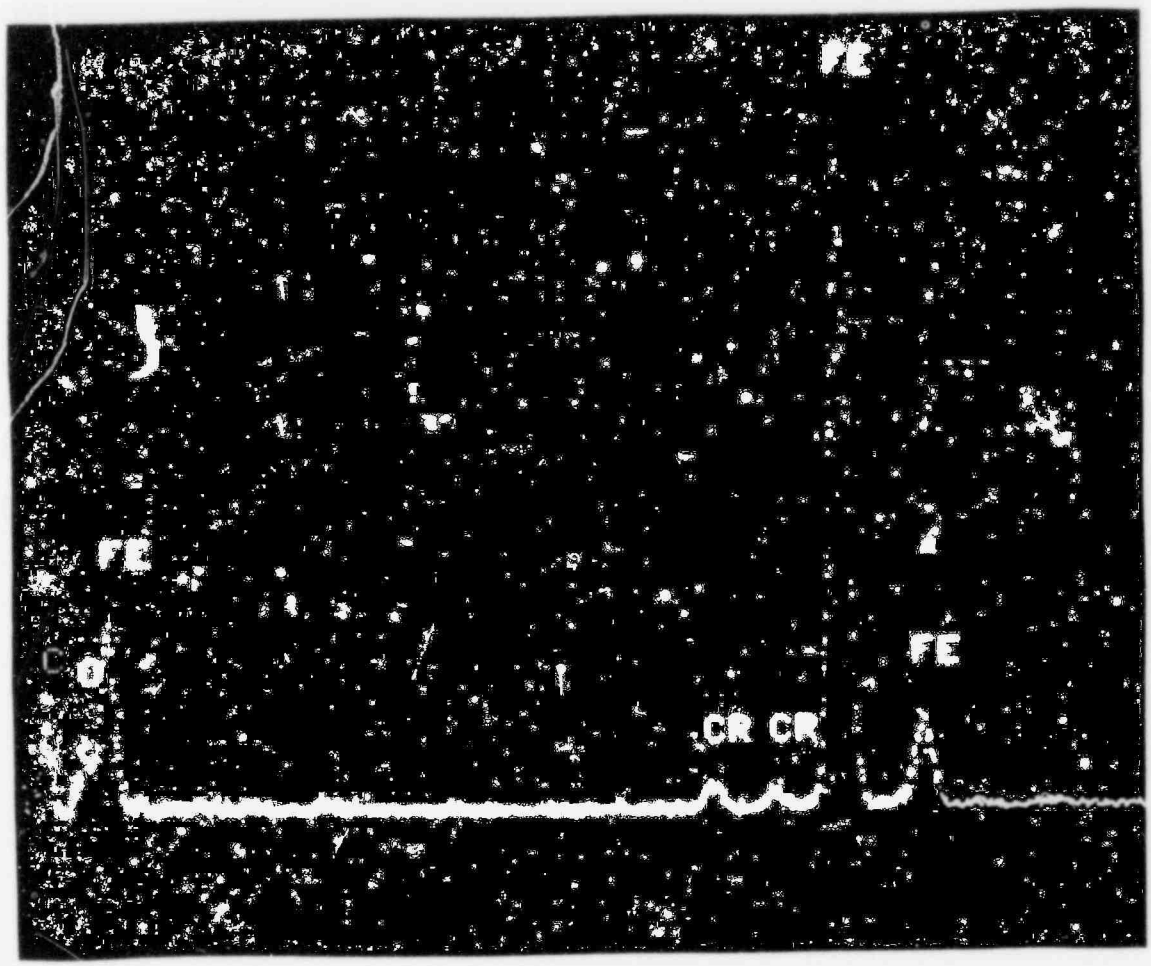

FIGURE HEDL-3. Energy-Dispersive X-Ray Spectrum from Electropolished A533 B Steel Showing Oxygen Peak Due to Surface Oxide.

characteristic compositions of second phase particles. Since the irradiated specimens contain the radioactive nuclide ^{55}Fe, which emits Mn characteristic X-rays in its decay by orbital electron capture, care was taken before analysis to strip appropriate activity spectra from the spectra obtained with the electron beam on the specimen.

3. Preparation for Annealing

As-received specimens were approximately 10 mm x 10 mm x 0.2 mm sheets. These were degreased, electropolished to remove surface contamination, and

3-mm diameter TEM disks were punched for the annealing studies. For annealing the specimens were sealed in quartz capsules that were evacuated and subsequently backfilled with 1/4 atmosphere of high purity argon.

Results

1. Microstructural Examination

As-received specimens (see Table HEDL-1) of KFA-1, 3, 4, and 5, covering a fluence range from 1.5×10^{18} n/c ^{2} to 7×10^{19} n/cm^2 and E>1 MeV, were prepared for TEM examination as described. No significant differences were found in the microstructures of these specimens. Individual grains varied in size from over 30 μm to less than 0.5 μm and contained recovered dislocation structures with well-defined dislocation sub-boundaries. Second phase particles 0.1 μm to 0.3 μm in diameter are common, as shown in Figure HEDL-4. Although the particles have similar morphologies, two predominant types were identified by electron diffraction and EDX analysis (see EDX analyses in Table HEDL-2). About 60% of the particles contain high molybdenum, and Mo_2C was identified by electron diffraction. However, the Mo content of these particles was highly variable, and it may be that M_6C or $(Fe_2Mo)C$ phases are also present. Most of the other particles were Fe_3C (cementite), characteristically containing about 11 wt. % Mn dissolved in the iron. Figure HEDL-4 also shows a characteristic single crystal diffraction pattern from an Fe_3C particle taken near a [001] matrix orientation. No distinct habit relationship between the Fe_3C and the ferrite matrix was evident. Figure HEDL-5 shows the dislocation structures at a low and a high fluence at high magnifications. Most of the background structure in Figure HEDL-5 is produced by surface oxides. The high fluence specimen KFA-5 also contained occasional small bubbles or void-like features. Electropolishing attack and "drop out" of small precipitate particles can cause such observations, although radiation-induced void or helium bubble formation is also a possibility.

POOR ORIGINAL

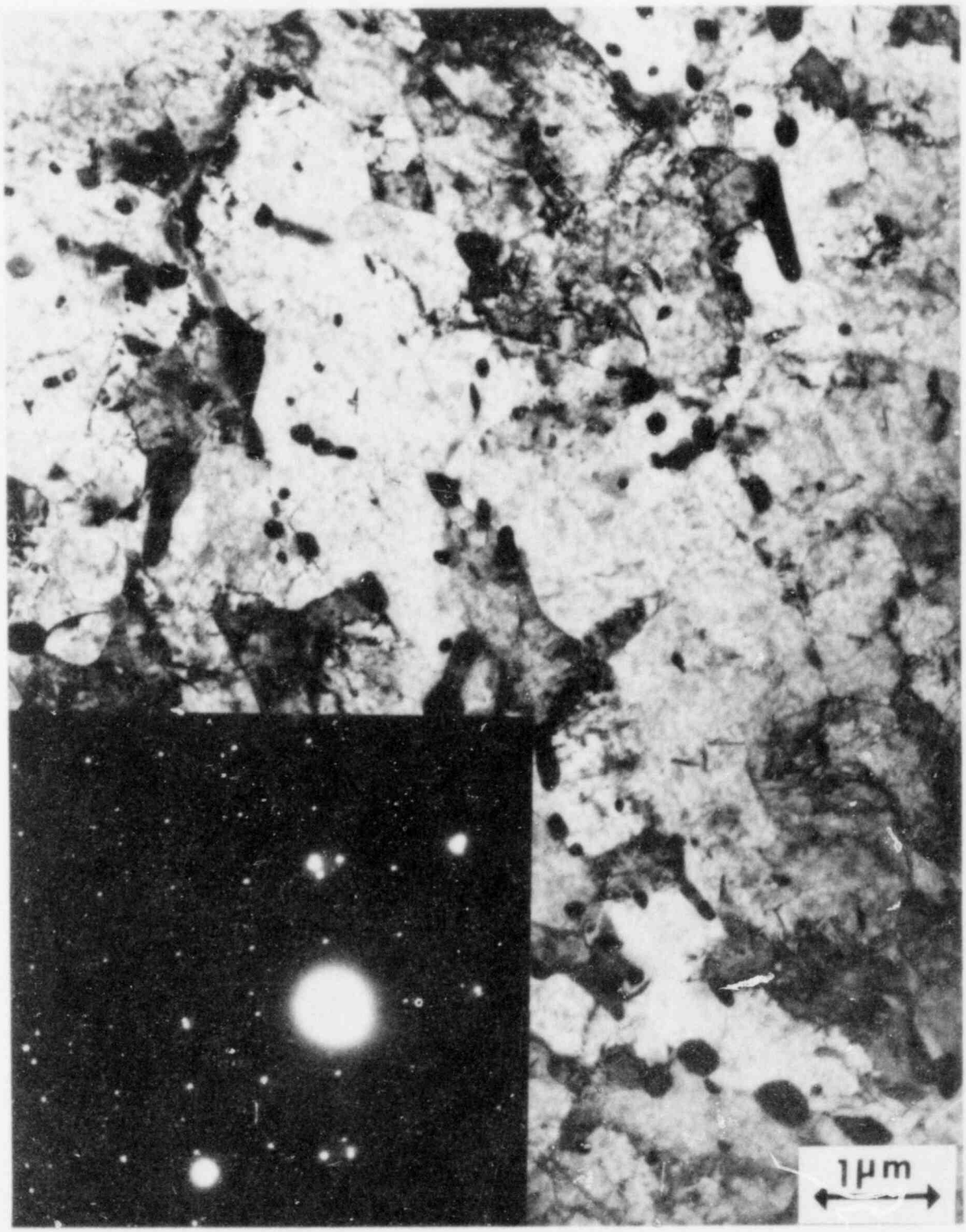

FIGURE HEDL 4. Microstructure of As-Received A533 B Steel (Specimen KFA-1). Prominent second-phase particles are Fe_3C (selected area diffraction pattern inset) and Mo_2C. (Photo Nos. 4629 and 4617).

TABLE HEDL-2

EDX MICROANALYSIS RESULTS: PRESSURE VESSEL STEEL A533 HSST 03 LF (WT. %)

	Al	Si	Cr	Mn	Fe	Ni	Mo	Number of Analyses (Averaged)
Overall Composition	<0.3	<0.3	1.1	1.6	95.2	0.7	0.8	5
Type A (Fe_3C) Precipitate	<0.3	<0.3	1.7	10.8	84.4	0.3	2.2	6
Type B (Mo_2C) Precipitate*	<0.3	<0.3	2.2	1.8	31.9	0.3	63.3	6
Type C Precipitate	3.5	0.3	1.8	1.7	60.5	0.3	31.9	1

* Mo:Fe ratio of Type B Precipitate highly variable (e.g., one particle contained 80% Mo, 15% Fe).

Discussion and Summary of Observations

Except for the unconfirmed observation of a few voids in A553 B steel irradiated at 7×10^{22} n/cm^2, E>1 MeV, none of the irradiated specimens show any visible indication of radiation-induced defects in the as-received condition. The presence of surface oxides formed during electropolishing precludes identification of such defects with sizes near the resolution limit for TEM. The predominant second phases, Fe_3C and Mo_2C, are those expected for this alloy composition.[3] An unexplained result is that the chromium composition indicated by EDX analysis for the A533 B Steel is significantly higher than that given by Pachur. This minor discrepancy lies well outside the uncertainty expected for the EDX analysis.

Expected Accomplishments

The work will continue with annealing and TEM examination of specimens.

POOR ORIGINAL

(a)

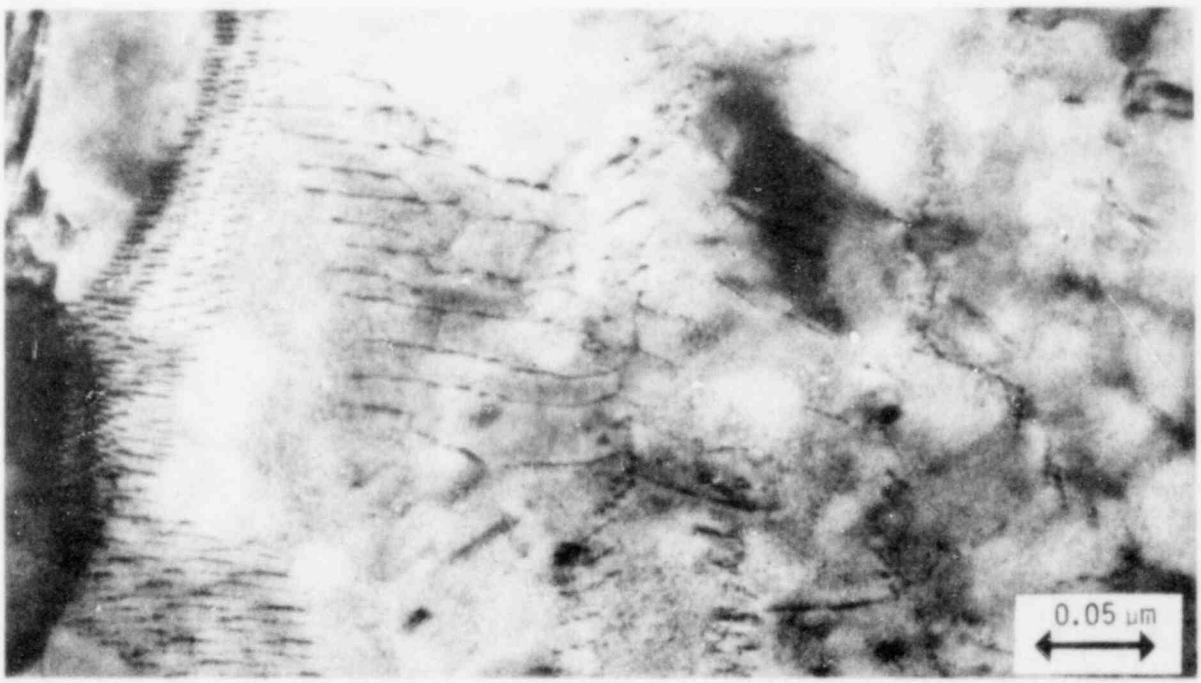

(b)

FIGURE HEDL-5 Dislocation Structure of Neutron-Irradiated A533 Steel. (a) KFA-1 (1.5×10^{18} n/cm), (b) KFA-4 (3×10^{19} n/cm^2, E>0.1 MeV). (Photo Nos. 4634 and 4626).

REFERENCES

1. J. A. Spitznagel, R. P. Shogun and J. H. Phillips, "Annealing of Irradiation Damage in High Copper Ferritic Steels," Irradiation Effects on the Microstructure and Properties of Steels, ASTM STP 611 pp. 434-448, 1976.

2. D. Pachur, "Embrittlement Saturation of Reactor Pressure Vessel Steels," Proceedings, NRC 7th Water Reactor Safety Research Information Meeting, National Bureau of Standards, Gaithersburg, MD, November 5-9, 1979.

3. K. W. Andrews, H. Hughes and D. J. Dyson, "Constitution Diagrams for Cr-Mo-V Steels," Journal of Iron & Steel Institute, Vol. 210, pp. 337-350, May, 1972.

B. REANALYSIS OF THE EXISTING DATA BASE RELATING IRRADIATION EMBRITTLEMENT AND NEUTRON EXPOSURE OF PRESSURE VESSEL STEELS.

G. L. Guthrie
R. L. Simons

Objective

The LWR Pressure Vessel Dosimetry Program is committed to the writing of ASTM standards relating irradiation induced embrittlement of pressure vessel steel and the relevant parameters associated with the exposure that produce embrittlement. These relevant parameters include the fluence, spectral shape, flux, irradiation temperature, and the chemistry, microstructure, and prior thermo-mechanical history of the steel being irradiated. The ultimate aim is to obtain analytic relations between the parameters and variables involved. The successful accomplishment of this task will require analysis of existing available data relating the embrittlement and the relevant parameters. The present report has the objective of analyzing the existing data base to ascertain the extent to which statistical scatter in the analytical relations can be reduced by the elimination of errors in the fluence calculations of previously reported experiments.

Summary

Nineteen surveillance reports from Westinghouse reactors were assembled as a first step in the reanalysis of the existing data relating irradiation induced embrittlement and neutron exposure for pressure vessel steels. A recalculation of the neutron exposure is proceeding for each of the reports. As a preliminary feasibility study, a method was devised to analyze a large data bank for characteristics in the data that are indicative of errors in the reported neutron exposure values. Analytic expressions relating Charpy shift to chemistry and exposure have standard deviations (uncertainties) that are partly due to errors in reported values of neutron exposure, and partly due to other sources or types of errors.

A way was found to estimate the contribution from neutron exposure errors. It appears that the standard deviation in Charpy shift formulas can be reduced significantly by removal of errors in neutron exposure value calculations. In some cases these errors are as large as a factor of two and result in an uncertainty of a factor of two for the safe operating life of the reactor.

In the course of the analysis, it was found that the least squares method of estimating the fluence exponent in Charpy shift formulas gave a biased value for the exponent with the least squares result being slightly low.

Accomplishments and Status

Nineteen surveillance reports for Westinghouse LWRs were collected and work is now in progress to check the dosimetry calculations for possible errors. Preliminary results on the recheck show errors of up to a factor of two in the reported values for the neutron exposure. The recheck values are based on the orginal counting data for the dosimeters, but have the benefit of revised values for activation cross sections, more recent results for spectral shape calculations as determined by the reactor design team, and improved unfolding procedures.

While the reports were being collected, a method was devised to check a large reactor surveillance data base for the symptoms of errors due to faulty dosimetry calculations. The basis of the method follows. The possible dosimetry calculation errors are nearly all of a type that causes the magnitude of the error to be proportional to the true value of the neutron exposure. That is, errors due to the use of an incorrect value for an activation cross section, or the use of an improper spectral shape, or the use of an improper unfolding technique all cause the reported neutron exposure to be in error by a multiplicative factor. Fluence calculation errors, which differed from one experiment to another or from one experimentor to another, would cause a random scatter in the total reported data, but the magnitude of the error would correlate with the magnitude of the observed shift in 30 ft-lb Charpy transition temperature.

The following plan was devised to ascertain the benefit obtained in removing the fluence calculation errors from the existing surveillance data. (1) We would examine a large collection of data to see if a "best fit" formula had discrepancies with the data where the magnitude of the discrepancy correlated with the magnitude of the Charpy shift. (2) We would manufacture Monte Carlo data by various means to determine the relation between various parameters and the correlation coefficient under study. (3) We would manufacture Monte Carlo data having all the known characteristics of the existing data base (same standard deviation, same correlation coefficient, same distribution of data points in fluence), and then turn off the "scatter" in the fluence and note any improvement in the standard deviation for a "best fit" analytic expression.

To implement this idea, a set of 144 data points was analyzed. The data was Charpy shift data from power reactor surveillance irradiations. The irradiated specimens included both plate and weld metal from a variety of alloys. This 144 point data set was analyzed using a least squares fitting procedure under the assumption that

$$\Delta NDTT = (A + B \cdot (\text{wt. \% Cu})) \cdot (\phi t)^{n} \qquad (1)$$

where ΔNDTT is the reported shift in the 30 ft-lb Charpy transition temperature, A, B, and n are adjustable parameters whose values are fixed by a least squares procedure, "wt. % Cu" is the reported weight per cent of copper in the PV steel, and t is the reported fluence (E>1.0 MeV). We define $\delta(\Delta NDTT)$ to be the difference between the reported value of ΔNDTT and that calculated from Equation (1). This difference was noted for each data point, and a correlation was calculated between the absolute value of $\delta(\Delta NDTT)$ and the reported Charpy shift, ΔNDTT. It was found that $|\delta(\Delta NDTT)|$ correlates with ΔNDTT with a correlation factor of 0.30 in the actual 144 point surveillance data set.

To ascertain the significance of the above observation, several additional calculations were made. First, a correlation was calculated between copper concentration and fluence to see if possible complications could arise from

such a phenomenon. The correlation coefficient was found to be only 0.07, which was regarded as being low enough so that any additional complications from that source could be ignored.

Then, using the "best" value for A, B, and n, and using the actual values for the reported fluence, the formula of Equation (1) was used together with a Monte Carlo routine to manufacture data where the "error" was all in the fluence and was all of a log-normal type. That is, starting with the reported fluence values, the "best" parameters of Equation (1) were used to generate a "correct" set of 144 values of ΔNDTT. Then, the 144 fluence values were shifted by a log-normal Monte Carlo generator. The new "noisy" fluence values were used with the 144 "correct" values of ΔNDTT, and this set was regarded as a set of manufactured data having log-normal "noise" in the fluence and zero "noise" in the 144 values for ΔNDTT. This manufactured data set was used to generate a new set of parameters for Equation (1) using a least squares technique, and a correlation coefficient was calculated for the correlation between $|\delta(\Delta NDTT)|$ and ΔNDTT. The coefficient was found to be approximately 0.6. The same value was found for the correlation coefficient whether

$$(\phi t)_{\text{Monte Carlo}} = (\phi t)_{\text{Reported}} \cdot \text{EXP}\left(\begin{matrix}\text{Normal Distribution} \\ \text{Centered at Zero}\end{matrix}\right) \qquad (2)$$

or

$$(\phi t)_{\text{Monte Carlo}} = (\phi t)_{\text{Reported}} \cdot \text{EXP}\left(1. + \left(\begin{matrix}\text{Normal Distribution} \\ \text{Centered at Zero}\end{matrix}\right)\right) \qquad (3)$$

was used for the law to generate the neutron exposures in the Monte Carlo data set. However in the case where Equation (3) was used, the standard deviation of the normal distribution had to be restricted to low values to

avoid obtaining negative values of fluence incompatible with the fractional exponent, n, in Equation (1).

Next, a Monte Carlo set of data was generated using 144 data points with a fluence distribution similar to the surveillance set, but with zero "noise" in the fluence and a normal distribution of noise in the Charpy measurement. The correlation between $|\delta(\Delta NDTT)|$ and $\Delta NDTT$ was approximately zero and gave small (~ 0.05) positive or negative values depending on the particular Monte Carlo set.

In view of the results above, it seemed that the overall analysis method had merit, and a set of Monte Carlo data was manufactured which had the following characteristics.

1. It was distributed in fluence similar to the distribution of the 144 data points of the surveillance data set.

2. It had a least squares fit with constants similar to those found for the 144 point surveillance data set.

3. The standard deviation of the fit matched that of the surveillance set. ($17^{o}C$)

4. The $|\delta(\Delta NDTT)|$ vs $\Delta NDTT$ correlation coefficient matched that of the surveillance set. (0.3)

5. The above characteristics were acquired by using a Monte Carlo generating technique with a log-normal noise generator for fluence noise and a normal noise generator for generation of errors in the measured value of $\Delta NDTT$. The general form of Equation (1) was used as the basis for the Monte Carlo technique. The input A, B, and n values, and also the two noise generator amplitudes, were adjusted to obtain the proper similarity to the 144 point surveillance data set.

After the above Monte Carlo set was acquired, the Monte Carlo generator was operated again with no change in controlling parameters except that the fluence noise generator amplitude was set to zero, simulating the removal of all errors in the fluence calculations. When the improved data was subjected to a least squares fit, the standard deviation of the errors in the fluence decreased by $4^{o}C$, from $17^{o}C$ to $13^{o}C$.

It should be noted that the indicated improvement is only that associated with the decrease in scatter about the curve of best fit, and does not take into account the shift between the two curves of best fit. Neither does it properly reflect the fact that some of the fluence data is in error by a factor of two with a possible consequent error of a factor of two in the calculated safe operating lifetime of an individual reactor.

One interesting feature which came out of the study was the following. When a proposed input law of the type shown in Equation (1), with particular values of A, B, and n was used to generate Monte Carlo data of the type described, the resultant output least squares value of n depended on the amplitude of the log-normal noise generator used to manufacture the data. That is, if the actual data has log-normal scatter in the fluence, a least squares fitting procedure gives a biased value for n in Equation (1). The bias increases with increasing log-normal scatter in the fluence. The least squares value for n is lower than the true value in the log-normal distribution. When a least squares value of 0.2775 is found for n as an output value, with a sigma of $17^{o}C$ and a correlation coefficient of 0.30, the actual input law has a value of n = 0.35. This bias phenomenon does not occur when the fluence data are distributed according to the law of Equation (3). Neither is the value of n affected by "normal" noise in ΔNDTT.

Expected Accomplishments in the Next Reporting Period

The reevaluation of the fluence values of the 19 surveillance reports is expected to be complete and the results of several calculations will be reported. These include the improvement in sigma for laws of the type shown in Equation (1), the maximum error in fluence ratios found in the reports, and the improvement to be obtained by using physically-based correlation laws containing saturation and annealing effects expressly written into the analytic expressions used in place of Equation (1).

OAK RIDGE NATIONAL LABORATORY
(ORNL)

A. NEUTRON FIELD CHARACTERIZATION-TRANSPORT CALCULATIONS

L. F. Miller
C. A. Baldwin
R. E. Maerker
J. J. Wagschal
G. Minsart (CEN/SCK)

Transport calculations to characterize the PSF neutron environment have been delayed to FY-81.

B. BENCHMARK FIELDS

L. F. Miller
F. B. K. Kam
L. P. Pugh

Objectives

The objectives of this task are: 1) to validate and guide neutron transport calculations for the LWR-PV program, 2) to establish well-characterized neutron environments for the validation of dosimetry and damage correlation techniques, and 3) to demonstrate the applicability of the results in reactor pressure vessel configurations. The results of this task will have a direct impact in the preparation of ASTM Standards for Surveillance of Light Water Reactor Pressure Vessels.

Summary

All scheduled differential and integral measurements at the PCA have been completed. The Westinghouse-HEDL perturbation experiment for a simulated Westinghouse surveillance has been completed at full power. Also, the design of the instrumentation and controls for the PSF was completed. Extensive testing of the surveillance capsule itself was conducted with largely good results.

Accomplishments and Status

At the PCA, fission chamber measurements were performed jointly by NBS and MOL personnel in the Blind Test 8/7 and 12/13 configurations. Final ^{237}Np fission rate traverses were obtained in the water positions in front of the thermal shield and in front of the pressure vessel simulator. Radiometric reaction rate measurements were made in the 12/13 configuration. This completes all scheduled differential and integral measurements at the PCA and no further measurements are anticipated for FY-80.

At the PSF, the Westinghouse-HEDL full-power perturbation experiment for a simulated Westinghouse surveillance capsule has been completed. The dosimeters from this experiment were separated in the hot cells and those belonging to HEDL were shipped. HEDL will be responsible for shipping the individual packets to the vendors and service laboratories. The CEN/SCK dosimeters were kept at ORNL for counting by A. Fabry and will be shipped to MOL.

Design of the instrumentation and controls for the PSF is completed, and the temperature signal leads have been connected to the "60% setback" of the ORR protection system.

During March, extensive testing of the surveillance capsule was conducted with the capsule temporarily positioned in the reactor pool. The tests basically fell into three categories. The first merely tested the integrity of the process instrumentation in its entirety from capsule to computer. The second was to determine capsule characteristics by raising the capsule's temperature profile to a steady-state by activating individual heaters within the capsule while simultaneously

recording system parameters. The capsule was then allowed to cool to ambient temperature while recording the cool-down rate. Capsule characteristics were then inputted to a mathematical model which computes thermodynamic constants for the model. These constants were incorporated into the control algorithm which had been developed in a general form for use in this project. After the algorithm was tailored for the surveillance capsule, the third series of tests was run. During this phase of testing, the capsule temperature was controlled successfully by the computer during several experiments at low temperatures (75°C). The algorithm performed well in that the temperature distribution was reasonably flat and within ±5°C limits.

Although the results from the automatic control tests were largely very good, one unexpected occurrence was a wide periodic shift in the heater duty cycles as computed by the algorithm to maintain the temperature has become stable. The algorithm will be reworked to dampen the duty cycle oscillation.

Expected Accomplishments in the Next Reporting Period

The experiment rig, complete with capsules, will be installed and operation will be started.

C. DOSIMETRY AND DAMAGE CORRELATION ANALYSIS

F. W. Stallmann
J. F. Eastham
A. Fabry (CEN/SCK)

Objective

The objective of this portion of the program is to obtain reliable information from dosimetry measurements and neutron transport calculations and to correlate the spectral parameters with structural changes in reactor componets. The information will be directly applicable to the preparation of several ASTM Practices for the LWR-PV Surveillance Program.

Summary

The following three tasks were performed during the report period:

1. Evaluation of measurements in the fourth NRC-HSST dosimetry experiment.
2. Evaluation of the dosimetry in the PCA 8/7 and 12/13 configuration for comparison with calculated values in the PCA Blind Test.
3. Evaluation of the results in the PCA calculational Blind Test.

Accomplishments and Status

The fourth NRC-HSST metallurgical experiment was interrupted because excessive heat was generated in the metallurgical sample due to gamma irradiation. A lead shield was installed to reduce gamma heating. The neutron fluxes in the new configuration were determined in a dosimetry experiment. The dosimetry capsules from the second HSST experiment were used. Neutron fluxes 1.0 MeV were determined using $^{103}Rh(n,n')^{103m}Rh$, $^{115}In(n,n')^{115m}In$, $^{58}Ni(n,p)^{58}Co$, and $^{27}Al(n,\alpha)^{24}Na$. The determination of fast fluxes in the new configuration is necessary in order to determine irradiation time for the metallurgical experiment. A detailed description is given in Appendix A.

A variety of fission chamber and foil dosimetry measurements were performed during 1978 and 1979 in the PCA 8/7 and 12/13 configurations. Through evaluation for the combined results, a set of absolute equivalent fission flux for several threshold reactions was derived. Absolute reaction rates for $^{235}U(n,f)$, both bare and cadmium covered, were also determined. An interim report of the evaluation is given in Appendix B. A major difficulty arose from the fluctuations in the absolute power levels of the PCA core and also from slight changes in the dimensions of the thermal-shield pressure-vessel configuration between 1978 and 1979. All known biases were compensated as best as possible, and the final absolute data should be accurate to ±7% (1σ). A detailed uncertainty analysis, including covariances information, will be performed later. The present set of measurements can be considered sufficiently reliable to be used as a basis for comparison in the calculation Blind Test.

The overall program for evaluating the results of the PCA calculational Blind Test is described in Appendix C. The data submitted by the participants have been transferred to DEC-10 disk storage. Some preliminary results are attached in Tables ORNL-MOL-1 through 4. A definite bias towards underestimation of fluxes can be observed for most of the participants, but the C/E ratio (calculation to experimental) falls substantially below 0.70 for only two participants. A comprehensive evaluation will be presented at the Blind Test Meeting at NBS on May 23, 1980.

Expected Accomplishments in the Next Reporting Period

Evaluation of the Blind Test results will be completed and presented at NBS on May 23, 1980. Evaluation of the PSF startup dosimetry will be completed. Results will be used to determine the irradiation time for the first SSC capsule.

Table ORNL-MOL-1. Calculated/Experimental Ratios for the $^{27}Al(n,\alpha)$ Reaction Based on Fission Equivalent Fluxes

Code Letters	Position				
	A1	PVF[a]	A4	A5	A6
		PCA 8/7 Configuration			
A	-	-	1.02	.98	.97
B1	-	-	1.14	1.16	1.15
B2	-	-	0.74	0.69	0.63
C	-	-	1.12	1.07	1.08
K	-	-	.93	.87	.85
Q	-	-	.84	.80	.80
R1	-	-	.37	.33	.30
R2	-	-	.34	.28	.27
S	-	-	.93	.82	.78
U	-	-	.72	.63	.57
Y	-	-	1.08	1.06	1.09
		PCA 12/13 Configuration			
A	1.00	1.10	1.04	1.00	.99
B1	1.04	-	1.10	1.10	1.15
B2	0.87	-	0.70	0.65	0.62
C	1.11	1.29	1.12	1.09	1.08
K	1.04	.94	.93	.89	.87
Q	.88	.88	.84	.82	.82
R1	.57	.47	.40	.34	.31
R2	.48	.40	.34	.30	.30
S	1.12	1.15	.86	.79	.75
U	.85	.86	.69	.60	.53
V	.73	1.07	1.04	.63	1.12
Y	1.02	1.28	1.17	1.15	1.17

[a]PVF - Pressure Vessel Front; position is 0.85 cm shifted towards core from position A3. Experimental values are adjusted accordingly.

Table ORNL-MOL-2. Calculated/Experimental Ratios for the $^{58}Ni(n,p)$ Reaction Based on Equivalent Fission Fluxes

Code Letters	Position				
	A1	PVF[a]	A4	A5	A6
		PCA 8/7 Configuration			
A	-	-	1.01	0.96	0.93
C	-	-	1.13	1.06	1.03
K	-	-	0.90	0.87	0.87
Q	-	-	0.69	0.79	0.76
R1	-	-	0.48	0.41	0.36
R2	-	-	0.43	0.36	0.34
S	-	-	0.84	0.74	0.68
U	-	-	0.86	0.82	0.79
Y	-	-	0.94	0.90	0.88
		PCA 12/13 Configuration			
A	1.04	1.13	1.04	0.99	0.99
C	1.15	1.36	1.14	1.09	1.09
K	1.16	0.98	0.95	0.93	0.97
Q	0.91	0.89	0.84	0.80	0.80
R1	0.73	0.59	0.49	0.42	0.38
R2	0.61	0.51	0.44	0.38	0.38
S	1.05	1.06	0.77	0.69	0.67
U	0.98	1.10	0.85	0.80	0.78
V	0.85	0.93	0.97	0.90	1.07
Y	0.94	1.13	0.98	0.95	0.96

[a]PVF - Pressure Vessel Front; position is 0.85 cm shifted to the core from position A3. Experimental values are adjusted accordingly.

Table ORNL-MOL-3. Calculated/Experimental Ratios for the $^{115}In(n,n')^{115m}In$ Based on Equivalent Fission Fluxes

Code Letters	Position				
	A1	PVF[a]	A4	A5	A6
		PCA 8/7 Configuration			
A	-	-	1.02	0.97	0.92
C	-	-	1.12	1.04	0.97
K	-	-	0.83	0.80	0.78
Q	-	-	0.73	0.74	0.67
R1	-	-	0.56	0.48	0.40
R2	-	-	0.49	0.42	0.38
S	-	-	0.85	0.77	0.71
U	-	-	0.86	0.83	0.79
Y	-	-	0.91	0.85	0.78
		PCA 12/13 Configuration			
A	1.00	1.04	1.10	1.07	1.05
C	1.11	1.27	1.21	1.16	1.11
K	1.15	0.90	0.95	0.94	0.94
Q	0.87	0.81	0.84	0.80	0.75
R1	0.78	0.60	0.57	0.51	0.44
R2	0.64	0.51	0.51	0.46	0.43
S	0.98	0.95	0.81	0.76	0.73
U	0.97	1.04	0.88	0.87	0.85
V	0.83	0.84	0.95	0.89	0.97
Y	0.91	1.03	0.99	0.95	0.91

[a]PVF - Pressure Vessel Front; position is 0.85 cm shifted to the core from position A3. Experimental values are adjusted accordingly.

Table ORNL-MOL-4. Calculated/Experimental Ratios for the $^{237}Np(n,f)$ Reaction Based on Equivalent Fission Fluxes

Code Letters	Position				
	A1	PVF[a]	A4	A5	A6
		PCA 8/7 Configuration			
A	0.92	0.93	0.98	0.98	0.95
C	0.99	1.02	1.08	1.05	0.99
K	0.76	1.02	1.73	0.73	0.71
Q	0.80	0.75	0.67	0.64	0.56
R1	0.82	0.71	0.59	0.54	0.47
R2	0.66	0.57	0.51	0.48	0.42
S	0.84	0.87	0.87	0.85	0.82
U	0.86	0.82	0.78	0.76	0.71
Y	0.84	0.83	0.85	0.82	0.75
		PCA 12/13 Configuration			
A	0.89	1.01	1.05	1.04	1.03
C	0.98	1.22	1.14	1.11	1.07
K	1.01	0.87	0.83	0.83	0.81
Q	0.77	0.77	0.75	0.71	0.66
R1	0.73	0.62	0.57	0.53	0.47
R2	0.60	0.53	0.51	0.49	0.45
S	0.85	0.90	0.81	0.80	0.79
U	0.85	1.00	0.79	0.77	0.73
V	0.74	0.78	0.81	0.75	0.81
Y	0.80	1.01	0.91	0.88	0.83

[a]PVF - Pressure Vessel Front; position is 0.85 cm shifted to the core from position A3. Experimental values are adjusted accordingly.

APPENDIX A

APPENDIX A

NEUTRONIC CHARACTERIZATION OF THE HEAVY SECTION STEEL TECHNOLOGY IT-CT CAPSULE A: PRELIMINARY RESULTS OF DOSIMETRY MEASUREMENTS IN THE CAPSULE A MOCKUP AT THE BSR

Our recommended values for the neutron flux >1 MeV at various experimental locations within the steel mockup in reference are given in Table 1, last column, at a BSR reactor core power of 2 MW. These data are estimated to be accurate to ±5%(1σ) or better.

The measurements have been performed by means of the two transportable NaI(Tl) spectrometers calibrated at the CEN/SCK Mol Cavity ^{235}U Thermal Fission Neutron Spectrum Standard Field. The methods and techniques are the same as applied to the neutron spectral characterization of the PCA Pressure Vessel Simulator. The good accuracy obtained stems largely from the use of this "Benchmark Field Referencing" approach. The directly observed experimental quantities, gathered in Table 2, are the equivalent fission fluxes for each selected dosimetry reaction, x:

$$\phi_f^x = \int_0^\infty \phi(E)\ \sigma_x(E)\ dE \,/\, \bar{\sigma}\ (\chi_{25}) \qquad (1)$$

where $\phi(E)$: neutron spectrum at given experimental location,

$\bar{\sigma}_x(\chi_{25})$: differential energy cross section for dosimeter x,

$\bar{\sigma}_x(\chi_{25})$: $\int_0^\infty \chi_{25}(E)\ \phi_x(E)\ dE$ (2)

with $\chi_{25}(E)$ the ^{235}U fission neutron spectrum.

Experimentally, ϕ_f^x =[activation ratio BSR/χ_{25}]$_x$ times [total flux in the Mol ^{235}U fission spectrum neutron field].

When using equation (1) to derive by transport theory calculations the ratios ϕ>1 MeV/ϕ_f^x, the denominator, equation (2), has been treated consistently with the numerator; e.g., the same energy group structure and group fluxes for χ_{25} have been used as in the source term of the discrete-ordinates analysis, and of course, σ_x(E) was also the same in both the numerator and denominator. The biases eliminated in this way are evidenced by a comparison of columns 2 and 3 in Table 3.

The ratios ϕ>1 MeV/ϕ_f^x in columns 4 to 6 of Table 3, times the equivalent fission fluxes in columns 2 to 5 of Table 2, provide the fluxes >1 MeV in columns 2 to 5 of Table 1.* It has been assumed that the neutron spectrum along the axis of a given, vertical experimental channel does not change with the distance to the capsule top; as shown by Table 4, this is true within experimental uncertainties, except very close to the edge (location 2.04 in. in center channel).

Figure 1 is a plot of the relative axial variation of the fast flux as function of distance to the capsule top. Complete documentation of this work, including an analysis of the uncertainties, will be prepared for future HSST progress report dissemination.

The results of the present measurements, after correction has been applied for the differences between the dosimetry mockup and the real metallurgical capsule, can be combined with in-situ neutron fluence measurements to provide an improved neutronic characterization of this HSST capsule. The values are listed in Table 5.

---

*Similar measurements by means of the ^{56}Fe(n,p)^{56}Mn reaction are not reported at this time because corrections for activation of manganese impurities, ^{55}Mn(n,γ)^{56}Mn, have not yet been assessed.

Table 1. Neutron Fluxes ϕ>1 MeV in HSST IT-CT Capsule A Mockup Derived from Equivalent Fission Flux Measurements and Transport Thoery Calculations

Experimental Location[a]	$^{103}Rh(n,n')^{103m}Rh$[b]	$^{115}In(n,n')^{115m}In$[b,c]	$^{58}Ni(n,p)^{58}Co$[b]	$^{27}Al(n,\alpha)^{24}Na$[b]	Recommended[b] Value
South Channel (0.5")					
16.5 in.	1.94(12)	2.17(12)	2.09(12)	2.17(12)	2.09(12)
11.0 in.	2.11	2.32	2.13	2.28	2.23
5.5 in.	1.59	1.77	1.68	1.74	1.70
Center Channel (2.0")					
13.04 in.	1.12	1.25(12)	1.23(12)	1.25(12)	1.21(12)
7.54 in.	9.93(11)	1.08	1.08	1.13	1.07(12)
2.04 in.	6.01(11)	7.13(11)	6.61(11)	7.15(11)	6.73(11)
East Channel					
16.5 in.	9.88(11)	1.02(12)	1.13(12)	1.21(12)	1.09(12)
11.0 in.	1.04(12)	1.28	1.20	1.27	1.20(12)
5.5 in.	8.12(11)	8.31(11)	9.07(11)	9.72(11)	8.81(11)

[a]The distances quoted (inches) are measured from the dummy capsule top.

[b]Neutron flux ϕ>1 MeV at a BSR core power of 2.0 MW; 2.03(12) typical means 2.03×10^{12} n/cm^2 × s

ORNL-MOL-A5

Table 2. Experimental Equivalent Fission Fluxes in HSST 1T-CT Capsule A Mock-up

Experimental Location[a]	$^{103}Rh(n,n')^{103m}Rh$[b]	$^{115}In(n,n')^{115m}In$[b,c]	$^{58}Ni(n,p)^{58}Co$[b]	$^{27}Al(n,\alpha)^{24}Na$[b]
South Channel				
16.5 in.	3.56(12)	2.80(12)	1.67(12)	1.53(12)
11.0 in.	3.86	3.00	1.75	1.61
5.5 in.	2.92	2.28	1.34	1.23
Center Channel				
13.04 in.	2.25(12)	1.58(12)	8.39(11)	7.45(11)
7.54 in.	2.00	1.36	7.37	6.70
2.04	1.21	9.01(11)	4.52	4.25
East Channel				
16.5 in.	1.97(12)	1.29(12)	7.80(11)	7.33(11)
11.0 in.	2.08	1.62	8.28	7.72
5.5 in.	1.62	1.05	6.26	5.89

[a] The distances quoted (inches) are measured from the dummy capsule top.

[b] Equivalent fission flux at a BSR core power of 2.0 MW.

[c] All indium data may be 4-5% high (see Table 1, footnote *c*).

ORNL-MOL-A6

Table 3. Dosimetry Parameters for HSST IT-CT Capsule A Mockup Analysis
(Transport Theory Data)

Reaction	Fission Spectrum Average Cross Section (mb)[a]		Calculated Ratio[c] [ϕ>1 MeV/Equivalent Fission Flux]		
	Experimental	Code[b]	South Channel	Center Channel	East Channel
$^{103}Rh(n,n')^{103m}Rh$	733	716	0.5455	0.4963	0.5013[e]
$^{115}In(n,n')^{115m}In$	189	168	0.7745	0.7912	0.7918[e]
$^{58}Ni(n,p)^{58}Co$	108.5	103.6	1.2518	1.4620	1.4496[e]
$^{27}Al(n,\alpha)^{24}Na$	0.705	0.854	1.4185	1.6813	1.6501[e]

[a] $\int_0^\infty \sigma(E)\, \chi_{25}(E)\, dE$ where $\chi_{25}(\#)$ is the ^{235}U thermal-induced fission neutron spectrum.

[b] XSDRNPM and DOT; χ_{25} is derived from ENDF/B-IV in a 12-group energy structure; except for Rh, the cross sections are from the ENDF/B-IV, dosimetry file.

[c] XSDRNPM one-dimensional transport theory.

[d] As in (c) but corrected using two-dimensional DOT calculation in which thermal shield between BSR core and present HSST capsule had been omitted.

[e] $\left(\frac{\text{Old value for east channel}}{\text{Old value for center channel}}\right) \times \left(\text{New value for center channel}\right) = \left(\text{New value for east channel}\right)$

Table 4. Integral Spectral Indices for HSST IT-CT Capsule A Mockup

Experimental Location[a]	$^{103}Rh(n,n')^{103m}Rh$[b] / $^{27}Al(n,\alpha)^{24}Na$	$^{115}In(n,n')^{115m}In$[b,d] / $^{27}Al(n,\alpha)^{24}Na$	$^{58}Ni(n,p)^{58}Co$[b] / $^{27}Al(n,\alpha)^{24}Na$
South Channel			
Exp.			
16.15 in.	2.33	1.83	1.09
11.0 in.	2.40	1.86	1.09
5.5 in.	2.37	1.85	1.09
Mean Exp.	2.37	1.85	1.09
Theory			
Dosimetry Capsule	2.60	1.83	1.14
Metall. Capsule	2.32	1.71	1.10
Center Channel			
Exp.			
13.04 in.	3.02	2.12	1.13
7.54 in.	2.98	2.03	1.10
2.04 in.	2.85	2.12	1.06
Mean Exp.[c]	3.00	2.08	1.11
Theory			
Dosimetry Capsule	3.36	2.11	1.14
Metall. Capsule	2.75	1.85	1.08

[a] The distances quoted (inches) are measjred from the dummy capsule top.

[b] Spedtral index or equivalent fission flux ratio.

[c] Data at 2.04 in. excluded.

[d] All indium data may be 4-5% high (see Table 1, Footnote c).

Calculated Integral Spectral Indices = $\dfrac{R.R._x / \text{Fission Spectrum Average x-Section x}}{R.R._y / \text{Fission Spectrum Average x-Section y}}$

Table 5. Final Estimates of Flux >1.0 MeV and >0.1 MeV at Different Locations in the Metallurgical Capsule

Distance from Capsule Face (cm)	Measurements and Calculations			
	Dosimetry Capsule		Metallurgical Capsule	
	ϕ(E) >1 MeV	ϕ(E) >.14 MeV	ϕ(E) >1 MeV	ϕ(E) >.14 MeV
0.3908	2.594(12)	8.382(12)	1.883(12)	5.479(12)
1.1723	2.279(12)	7.811(12)	1.651(12)	5.087(12)
1.9538	2.008(12)	7.251(12)	1.464(12)	4.642(12)
2.7354	1.767(12)	6.707(12)	1.285(12)	4.283(12)
3.5169	1.555(12)	6.183(12)	1.115(12)	3.836(12)
4.2985	1.367(12)	5.679(12)	9.726(11)	3.453(12)
5.0800	1.200(12)	5.193(12)	8.342(11)	3.033(12)
5.8615	1.051(12)	4.723(12)	7.182(11)	2.659(12)
6.6431	9.182(11)	4.269(12)	6.112(11)	2.320(12)

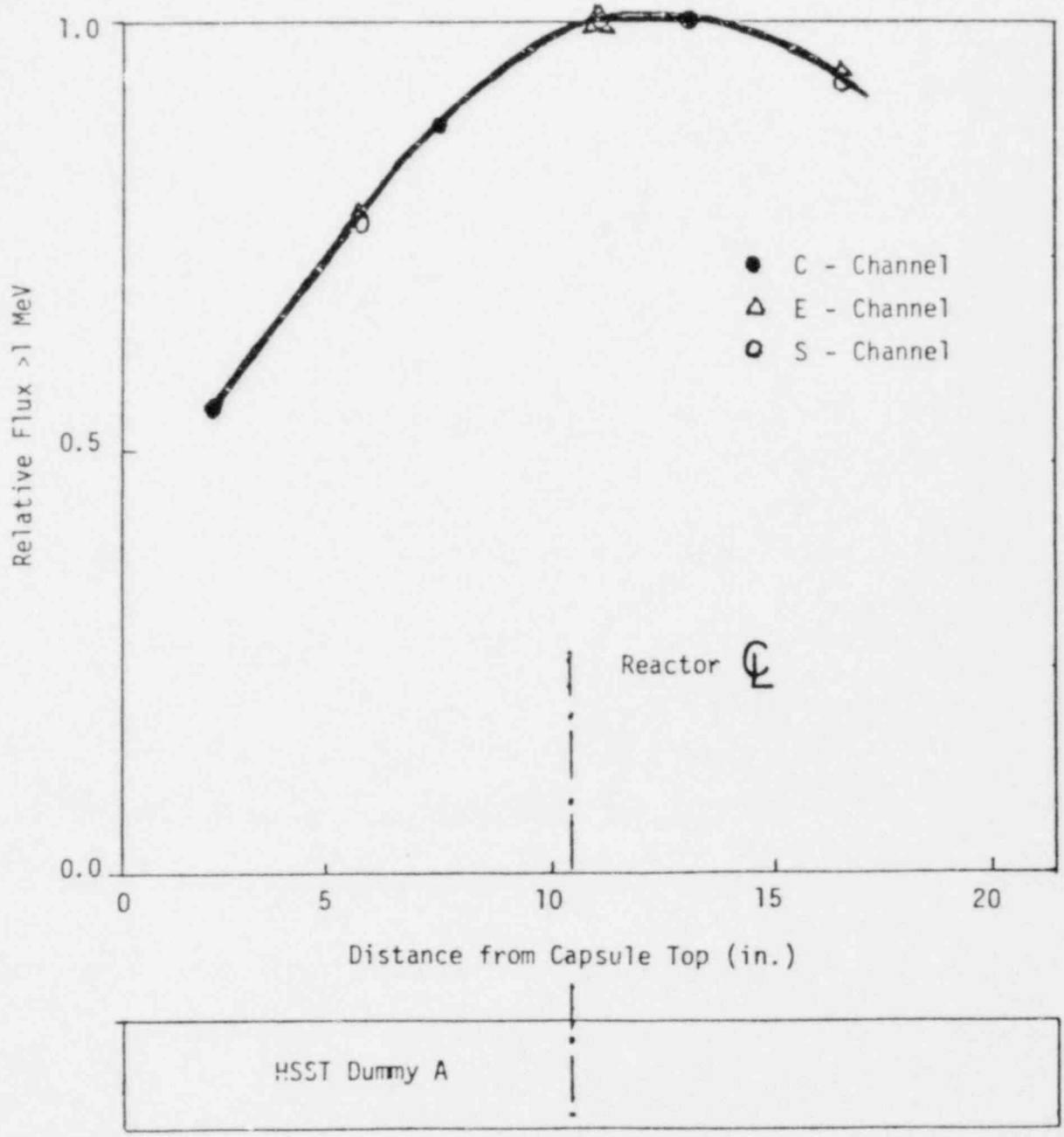

Fig. 1. Relative Flux Distribution in the Dummy HSST Capsule at BSR. (Axial Shape Vertical)

APPENDIX B

APPENDIX B

RELEASE OF EXPERIMENTAL DATA FOR THE VALIDATION OF THE PCA BLIND TEST CALCULATIONS

A. Fabry (CEN/SCK), E. D. McGarry (NBS)

This is an interim release of experimental data obtained in the PCA 8/7 and 12/13 configurations for comparison with calculations for the Blind Test. The data are based on radiometric and fission chamber measurements by A. Fabry, CEN/SCK, MOL, Belgium, and E. D. McGarry, NBS. Data from other experimenters have not yet been included pending further evaluation and intercomparison. Also, many other data from the above laboratories will be released at a later date, especially the data at the A1 and A2 positions in the 8/7 configuration and the $^{235}U(n,f)$ reactions. Some of the additional data will be available at the Blind Test meeting at NBS, May 22-23, 1980.

All measurements are made relative to a calibrated U-235 fission field at NBS or MOL respectively. This procedure reduces or eliminates completely many of the uncertainties in the counting equipment like absolute efficiency, or nuclear constants like branching ratios. The resulting quantities are expressed as "equivalent fission fluxes" and presented in Table 1. To convert these data to absolute reaction rates, the equivalent fission fluxes must be multiplied with the average reaction cross section of the target nuclide in the U-235 fission spectrum. Experimental average cross sections are listed below. These were applied to convert the data in Table 1 to the absolute reaction rates in Table 4. As an alternative, calculated average cross sections may be used which are derived from the fission field and cross section file for Blind Test calculations. This reduces the uncertainties in the source spectrum and cross section file which enter the calculations of the absolute reaction rates.

The combined (in the sum of squares sense) uncertainties of the equivalent fission fluxes in Table 1 are ≈ ±7% (1σ), except as noted. The major sources of experimental uncertainties (1σ) are as follows:

1. Experimental precision, like counting statistics, deadtime and background corrections, corrections for interfering reactions, run-to-run monitoring, lateral positioning — < ±2%
2. Instrument calibration by reference irradiations in the NBS of Mol Cavity U-235 fission spectrum standard field — ±3.5-4.0%
3. Measurement of the PCA reactor core power based on: $\bar{\nu} = 2.4192$
   watts per fission $= 3.204 \cdot 10^{-11}$
   (This conversion factor is common to all measurements) — ±4.1%
4. Uncertainties due to the dimensions of the PCA experimental configuration (a slight change in the configuration occurred between 1978 and 1979/80 measurements and has been corrected for) — ±1.8%
5. Neutron field instrumental perturbation (not corrected)
   in water — ±3.0%
   in steel — ±0.5%

Not corrected were errors due to photon-induced reactions. Preliminary correction factors are listed in Table 3.

The experimental average reaction cross sections in the U-235 fission spectrum are as follows:

$^{237}Np(n,f)$ F.P.	1312 ± 50 mb
$^{103}Rh(n,n)^{103m}Rh$	733 ± 38 mb
$^{115}In(n,n)^{115m}In$	189 ± 8 mb*
$^{238}U(n,f)$ F. P.	305 ± 9 mb
$^{58}Ni(n,p)^{58}Co$	108.5 ± 5.4 mb
$^{27}Al(n,\alpha)^{24}Na$	0.705 ± 0.040 mb

Direct measurements of the ratios of $^{237}Np(n,f)/^{238}U(n,f)$ equivalent fission fluxes through NBS fission chambers are listed in Table 2. These "spectral indices" have much higher accuracies than single measurements as indicated in this table. This measurement serves as an indicator for the shape of the spectrum.

A more detailed description of the measuring techniques and uncertainties will be provided at the Blind Test meeting.

*The branching ratio for the ^{115m}In 336.2 keV gamma ray is 45.9%. This deviates from the value of 50% on which the ENDF/B-IV cross sections are based. The calculated average cross section, using ENDF/B-IV, is 168 mb.

Table 1. PCA Equivalent Fission Fluxes Per Unit Core Neutron Source Strength

Blind Test Specification	Experimental Specification[a]	$^{237}Np(n,f)$	$^{103}Rh(n,n')$	$^{115}In(n,n')$	$^{238}U(n,f)$	$^{58}Ni(n,p)$	$^{27}Al(n,\alpha)$
			PCA 8/7 Configuration				
A1	TSF	1.41(-5)	-	-	-	-	-
A2	PVF[a]	1.65(-6)	-	-	-	-	-
A4	1/4 T	5.74(-7)	4.68(-7)	3.37(-7)	3.39(-7)	2.40(-7)	3.57(-7)
A5	1/2 T	3.17(-7)	2.54(-7)	1.59(-7)	1.46(-7)	9.39(-8)	1.42(-7)
A6	3/4 T	1.68(-7)	1.29(-7)	7.09(-8)[b]	6.13(-8)	3.41(-8)	5.20(-8)
A7	VB	-	3.67(-8)	1.77(-8)[c]	-	-	1.46(-8)[c]
			PCA 12/13 Configuration				
A1	TSF	6.54(-6)	5.42(-6)	5.50(-6)	-	5.68(-6)	7.80(-6)
-	PVF[a]	2.30(-7)	2.02(-7)	1.97(-7)	-	2.26(-7)	4.46(-7)
A4	1/4 T	9.18(-8)	7.65(-8)	5.81(-8)	6.27(-8)	5.18(-8)	1.02(-7)
A5	1/2 T	5.12(-8)	4.10(-8)	2.70(-8)	2.76(-8)	2.05(-8)	4.10(-8)
A6	3/4 T	2.67(-8)[b]	2.08(-8)	1.17(-8)	1.14(-8)	7.29(-9)	1.53(-8)
A7	VB	8.01(-9)[b]	-	-	-	-	-

Data are not corrected for photon-induced responses (see Table 3). Total experimental uncertainty for all data (random and systematic) ±7% (1σ) except as noted in footnotes *b* and *c* with total uncertainties of ±9% and ±12% respectively.

[a]TSF - Thermal Shield Front
PVF - Pressure Vessel Front (this position is 0.85 cm closer to the PCA reactor core than the position A3 in the "Blind Test" specifications; this coincides with A2 in the PCA 8/7 configuration.

[b]Experimental precision ±5-6% (1σ).

[c]Experimental precision ±10% (1σ).

ORNL-MOL-86

Table 2. Benchmark Referenced Spectral Indexes for $^{237}Np/^{238}U$ in the Reactor Pressure Vessel (RPV) Simulator at the ORNL PCA

	Position Within the RPV Simulator	Observed and ETZ & DT Corrected Ratios of Fission Count Rates in PCA[1]	Corrections for Fissions in Impurities	Observed Ratios Adjusted for Fissions in Impurities See Note[2] About Uncertainties	Calibration Factor: Measured Ratios of Count Rates in CF-252 Neutron Field	Spectral Indexes in PCA Relative to Those in CF-252	Spectral Indexes in PCA As Derived from Relative Indexes	Spectral Indexes in PCA Relative to Those in U-235[3]
8/7 Configuration	1/4 T	2.895±0.89%	$\frac{0.997(2)}{1.000(1)}$	2.89±0.92%		1.75±1.74%	7.32±3.0%	1.68±2.6%
	1/2 T	3.70±1.05%	$\frac{0.997(2)}{1.000(1)}$	3.69±1.07%	1.650 ±0.41%	2.24±1.83%	9.36±3.2%	2.15±2.7%
	3/4 T	4.64±1.48%	$\frac{0.997(2)}{1.000(1)}$	4.63±1.50%		2.81±2.11%	11.7±3.3%	2.70±2.9%
12/13 Configuration	1/4 T	2.51±0.94%	$\frac{0.998(2)}{1.000(1)}$	2.51±0.97%		1.52±1.77%	6.35±2.8%	1.46±2.7%
	1/2 T	3.22±1.21%	$\frac{0.998(2)}{1.000(1)}$	3.21±1.23%	1.650 ±0.41%	1.94±1.92%	8.11±2.9%	1.86±2.8%
	3/4 T	4.06±1.62%	$\frac{0.997(2)}{1.000(1)}$	4.05±1.64%		2.45±2.21%	10.2±3.1%	2.35±3.1%

[1] Ratios of ETZ and DT corrected $\langle S_u \rangle$ values above 36/100 of the peak of the observed fission-product pulse-height distribution; units of per sec.

[2] Uncertainties of 0.7% must be added to account for uncertainty in configuration geometry; 1.2% because scattering in Cd + chamber assumed same in PCA and Cf; 0.3% possible void perturbation.

[3] Given for reference only.

[4] These data have not been corrected for photofission. Also no uncertainty added for this. Results are derived from the relative indexes times 4.18 ± 2.2%.

ORNL-MOL-87

Table 3. Gamma-To-Neutron Response Fractions in the PCA "Blind Test" Configuration

Blind Test Specification	Experimental Specification[a]	$^{237}Np(n,f)$	$^{103}Rh(n,n')$	$^{115}In(n,n')$	$^{238}U(n,f)$
		PCA 8/7 Configuration			
A1	TSF	0.9%	<0.5%[c]	0.2%	2.1%
A2	PVF	3.0%	<0.5%	0.8%	7.7%
A4	1/4 T	0.9%	<0.5%	0.4%	3.5%
A5	1/2 T	0.4%	<0.5%	0.2%	2.2%
A6	3/4 T	1.2%	<0.5%	0.8%	7.9%
		PCA 12/13 Configuration			
A1	TSF	1.1%	<0.5%[c]	0.3%	2.7%
-	PVF[b]	5.9%	<0.5%	1.3%	13.1%
A4	1/4 T	1.9%	<0.5%	0.7%	6.7%
A5	1/2 T	0.8%	<0.5%	0.4%	3.5%
A6	3/4 T	1.1%	<0.5%	0.6%	6.0%

Coupled Neutron-Gamma Transport Theory Calculations: G. Minsart (MOL)
Convolution of Neutron and Gamma Spectra with Photofission and γ,γ' Cross Sections: C. Eisenhauer (NBS)

[a] See Table 1 for explanation.

[b] Interpolated from calculations.

[c] Rough estimate.

Table 4. PCA Experimental Absolute Reaction Rates Per Unit Core Neutron Source Strength

Blind Test Specification	Experimental Specification[a]	$^{237}Np(n,f)$	$^{103}Rh(n,n')$	$^{115}In(n,n)^{b}$	$^{238}U(n,f)$	$^{58}Ni(n,p)$	$^{27}Al(n,\alpha)$
			PCA 8/7 Configuration				
A1	TSF	1.85(-29)	-	-	-	-	-
A2	PVF[a]	2.16(-30)	-	-	-	-	-
A4	1/4 T	7.53(-31)	3.43(-31)	6.37(-32)	1.03(-31)	2.60(-32)	2.52(-34)
A5	1/2 T	4.16(-31)	1.86(-31)	3.01(-32)	4.45(-32)	1.02(-32)	1.00(-34)
A6	3/4 T	2.20(-31)	9.46(-32)	1.34(-32)	1.87(-32)	3.70(-33)	3.67(-35)
A7	VB	-	2.69(-32)	3.35(-33)	-	-	1.03(-35)
			PCA 12/13 Configuration				
A1	TSF	8.58(-30)	3.9?(-30)	1.04(-30)	-	6.16(-31)	5.50(-33)
-	PVF[a]	3.02(-31)	1.48(-31)	3.72(-32)	-	2.45(-32)	3.14(-34)
A4	1/4 T	1.20(-31)	5.61(-32)	1.10(-32)	1.91(-32)	5.62(-33)	7.19(-35)
A5	1/2 T	6.72(-32)	3.01(-32)	5.10(-33)	8.42(-33)	2.22(-33)	2.89(-35)
A6	3/4 T	3.50(-32)	1.52(-32)	2.21(-33)	3.48(-33)	7.91(-34)	1.08(-35)
A7	VB	1.05(-32)	-	-	-	-	-

Data are not corrected for photon-induced responses (see Table 3).

[a]See Table 1 for explanation.

[b]Branching ratio for the ^{115m}In 336.2 keV gamma ray: 45.9% (see text).

APPENDIX C

APPENDIX C

The first task will be the transfer of the Blind Test data to disk files in the DEC-10 system for easy access and further manipulation. Since there is a fairly large volume of data, it is planned to first transfer the data directly to punch cards in the same format as they are submitted by the Blind Test participants. Editing and formatting can then be done through the DEC-system.

The data submitted by the Blind Test participants consist of:

1. Absolute reaction rates for a given set of about 10-12 foil detectors calculated at 6-8 experimental positions for each of the 8/7 and 12/13 configurations.

2. Calculated fluxes for E >1 MeV and E >0.1 MeV at experimental positions.

3. Calculated neutron flux spectra at all experimental positions given as group fluxes in energy group structures selected by the participants. These structures contain between 17 and 171 energy groups.

4. The source fission spectrum used in the calculation, usually given by the participants in their energy group structure.

In addition, experimental data from measurements in the PCA will be used for comparison with calculated data. The primary source of experimental data are fission chamber and radiometric measurements. These will be given primarily as benchmark referenced data in reference to standard fission fields at NBS and CEN/SCK. Absolute reaction rates will be provided using the fission flux spectrum at the reference field. Alternatively, calculated fission spectrum referenced data will be generated for direct comparison using the source fission spectra which are used by the participants. Results from neutron spectroscopy measurements will also be included as far as these data become available. All experimental data will be provided with appropriate uncertainty bounds.

Computer programs will be written (or existing ones, like WINDOWS, will be used) to generate the following summaries and tables:

1. Comparison of calculated absolute reaction rates between the different participants, including some measure for the spread of the results.

2. Comparison of selected spectral indices, e.g., $^{237}Np(n,f)/^{238}U(n,f)$.

3. Comparison of the calculated attenuations of the fluxes through water and steel (lead factors), expressed for instance, as the ratio between experimental position A2 (surveillance) and A4 (1/4 thickness) for typical reaction rates.

4. Summaries 1-3 will also be provided in the form of C/E (calculated to experimental) ratios instead of calculated values alone. The C/E ratios will be either given in regard to the absolute reaction rates or to benchmark referenced data as outlined above.

5. For comparison of the spectral shapes, the neutron spectra in the participants group structure will first be converted to 621 point spectrum which are continuous and consistent with the original group flux representations. These point spectra can either be compared directly or suitably collapsed to a selected (say 40 group) energy structure. The WINDOW program has all necessary provisions for carrying out this procedure.

6. The procedure in 5 can also be used to generate absolute reaction rates from cross section files other than the ones used by the participants for a more uniform comparison of these data.

7. If available, neutron spectroscopy data will be used for comparison with calculated spectra using the procedure in 5.

Further ideas concerning the comparison of the Blind Test results will undoubtedly develop during the course of evaluation. It is expected that most ideas can readily be implemented once the results from the participants are stored in an easily accessible and consistent format.

DISTRIBUTION

R5 (375)

DOE/FFTFPO (5)
P.O. Box 550
Richland, WA 99352

AR DeGrazia (4)
TL King

DOE/RRT-HQ (2)
Mail Stop B-107
Washington, DC 20545

Chief, Reactor Physics Branch
JW Lewellen

AERE HARWELL (2)
Oxfordshire OX11 ORA
UNITED KINGDOM

LM Davies
AJ Fudge

AERE WINFRITH (4)
Dorchester, Dorset

J. Butler
CG Campbell
AK McCracken
J. Sanders

ARGONNE NATIONAL LABORATORY (1)
9700 South Cass Avenue
Argonne, II 60439

Roland J. Armani
Building 316

BABCOCK & WILCOX (1)
Lynchburg Research Center
P.O. Box 1260
Lynchburg, VA 24505

RH Lewis

DISTRIBUTION (Cont'd)

BATTELLE-COLUMBUS (2)
505 King Avenue
Columbus, OH 43201

D. Farmelo
J. Perrin

BROOKHAVEN NATIONAL LABORATORY (3)
National Neutron Cross Section Center
Upton, NY 11973

JF Carew
BA Magurno
Pearlstein, Building T-197

CENTRE D'ETUDES NUCLEAIRES de SACLAY (3)
B. P. No. 2
91190 Gif sur Yvette
FRANCE

AA Alberman
JM Cerles
JP Genthon

CENTRE D'ETUDE de l'ENERGIE NUCLEAIRE (4)
Boeretang 200
Mol, Belgium

J. Debrue
G. DeLeeuw
S. DeLeeuw
A. Fabry

COMBUSTION ENGINEERING (1)
1000 Prospect Hill Road
Windsor, CT 06095

J. Varsik

COMMONWEALTH EDISON (1)
P.O. Box 767
Chicago, IL 60690

AD Rossin

EG&G IDAHO, INCORPORATED (3)
P.O. Box #1625
Idaho Falls, ID 83401

R. Greenwood
Y. Harker
JW Rogers

ELECTRIC POWER RESEARCH INSTITUTE (5)
3412 Hillview Avenue
P.O. Box 10412
Palo Alto, CA 94304

T. Marston
O. Ozer
FJ Rahn
K. Stahlkopf
HA Till

EURATOM (3)
JRC Ispra
I 21020 Ispra (VA)
ITALY

R. Dierckx

Comitato Nazionale Per L'Energie Nucleare
Centro Di Studi Nucleari Della Casaccia
Casella Postale 2400
00060 Santa Maria di Galeria
Rome, Italy

U. Farinelli

ECN Netherlands Energy Research Foundation
Weterduinweg 3
Petten, (N.H.)
NETHERLANDS

WL Zijp

FRACTURE CONTROL CORPORATION (1)
330 South Kellogg Avenue
Suite E
Goleta, CA 93017

RA Wullaert

GENERAL ELECTRIC COMPANY (1)
Vallecitos Nuclear Center
P. O. Drawer B
Vallecitos Road
Pleasanton, CA 94566

GC Martin

INTERNATIONAL ATOMIC ENERGY AGENCY (2)
Karntner Ring 11
P. O. Box 590
A-1011 Vienna
AUSTRIA

V. Chernyshev
J. Schmidt

IKE - STUTTGART (1)
Postfach 801140
7000 Stuttgart-80 (Vaihingen)
PFAFFENWALDRING 31
WEST GERMANY

G. Prillinger

IRT CORPORATION (3)
P.O. Box 80817
San Diego, CA 92183

NA Lurie
C. Preskitt
WE Selph

KFA - ZBB
Kernforschungsanlage Julich Gmbh (2)
Postfach 1913
D-5170 Julich 1
WEST GERMANY

D. Pachur
W. Schneider

LOS ALAMOS SCIENTIFIC LABORATORY (2)
University of California
P.O. Box 1663
Los Alamos, NM 87544

G. Hansen, Group N-2
L. Stewart

MACALESTER COLLEGE (1)
Dept. of Physics & Astronomy
St. Paul, MN 55105

JH Roberts

NATIONAL BUREAU OF STANDARDS (4)
Center of Radiation Research
U.S. Department of Commerce
Washington, DC 20234

RS Caswell
CM Eisenhauer
JA Grundl
ED McGarry

NAVAL RESEARCH LABORATORY (3)
Thermostructural Materials Branch
Code 6392
Engineering Materials Division
Washington, DC 20375

Code 6653
R. Hawthorne
M. Rosen
L. Steele

NUCLEAR REGULATORY COMMISSION (13)
Metallurgy & Materials Research Branch
Mail Stop SS-1130
Washington, DC 20555

Chief
Public Document Room (3)
M. Bolotski
M. Dunenseld
R. Gamble
W. Hazelton
L. Lois
S. Pawlicki
PN Randall
CZ Serpan
D. Sieno

DISTRIBUTION (Cont'd)

OAK RIDGE NATIONAL LABORATORY (17)
P.O. Box Y
Oak Ridge, TN 37830

RG Berggren
CD Cagle
DA Canonico
JA Conlin
JA Cox
RM Freestone, Jr.
SS Hurt
FB K. Kam
RE Maerker
RV McCord
LF Miller
FR Mynatt
F. Perey
I. Siman-Tov
FW Stallmann
JH Swanks
CR Weisbon

ORTEC, INC. (1)
100 Midland Road
Oak Ridge, TN 37830

W Zimmer

PACIFIC NORTHWEST LABORATORY (2)

WC Morgan
Materials Department
PSL Building/Room 1303
Richland, WA 99352

CA Oster
Engineering Physics Department
Math Building/Room 1248
Richland, WA 99352

RADIATION RESEARCH ASSOCIATES (2)
3550 Hulen Street
Ft. Worth, TX 76107

RM Rubin
MB Wells

ROCKWELL INTERNATIONAL ENERGY SYSTEMS GROUP (2)
P.O. Box 309
Canoga Park, CA 91304

HA Farrar IV
B. Oliver

ROLLS-ROYCE & ASSOCIATES LIMITED (2)
P.O. Box No. 31
Derby, England

M. Austin
P. Burch

SCIENTIFIC APPLICATIONS INCORPORATED (3)
1200 Prospect Street
LaJolla, CA 92037

W. Hagan
L. Simmons
VV Verbinski

SOUTHWEST RESEARCH INSTITUTE (1)
8500 Culebra Road
P.O. Box 28510
San Antonio, TX 78284

EB Norris

UNIVERSITY OF CALIFORNIA SANTA BARBARA (1)
Department of Chemical & Nuclear Engineering
Santa Barbara, CA 93106

GR Odette

UNIVERSITY OF TOKYO (2)
Dept. of Nuclear Engineering
7-3-1, Hongo
Bunkyo-ku, Tokyo
JAPAN

M. Nahazawa
J. Sekiguchi

WESTINGHOUSE ELECTRIC CORPORATION (7)
Advanced Nuclear Systems Division
P.O. Box 355
Pittsburgh, PA 15230

S. Anderson
J. Davison
TR Mager
JJ Taylor
SE Yanichko

Research Division
P.O. Box 355
Pittsburgh, PA 15230

R. Holland
JA Spitznagel

HANFORD ENGINEERING DEVELOPMENT LABORATORY (36)
Supervisor, Document Processing
P. O. Box 1970
Richland, WA 99352

HJ Anderson	W/C-39	WN McElroy	W/C-33
RA Bennett	W/B-43	PA Ombrellare	W/C-45
TK Bierlein	W/A-57	LM Osland	W/C-115
WL Bunch	W/B-47	FH Ruddy	W/C-39
LL Carter	W/B-47	RE Schenter	W/A-4
DG Doran	W/A-57	FA Schmittroth	W/A-4
DS Gelles	W/A-57	WF Sheely	W/A-62
R. Gold	W/C-39	EM Sheen	W/A-56
GL Guthrie	W/C-39	RL Simons	W/A-57
JJ Holmes	W/A-58	JA Williams	W/A-40
LA James	W/A-40	HH Yoshikawa	W/A-44
BJ Kaiser	A/A-56	Central Files (2)	
LS Kellogg	W/C-39	Program Files (5)	
RL Knecht	W/A-40	c/o WN McElroy	W/C-39
EP Lippincott	W/C-39	Publ. Services (2)	W/C-115
WY Matsumoto	W/C-33		

NRC Form 335

U.S. NUCLEAR REGULATORY COMMISSION

BIBLIOGRAPHIC DATA SHEET

1. REPORT NO.: NUREG/CR-1241, Vol. 1
HEDL-TME-80-4

2. (Leave blank)

3. RECIPIENT'S ACCESSION NO.

4. TITLE AND SUBTITLE (Add Volume No., if appropriate)
LWR Pressure Vessel Irradiation Surveillance Dosimetry
Quarterly Progress Report: January - March 1980

5. DATE REPORT COMPLETED
MONTH: August YEAR: 1980

DATE REPORT ISSUED
MONTH: December YEAR: 1980

6. (Leave blank)

8. (Leave blank)

7. AUTHOR(S)
G. L. Guthrie and W. N. McElroy

9. PERFORMING ORGANIZATION NAME AND MAILING ADDRESS (Include Zip Code)
Hanford Engineering Development Laboratory
P.O. Box 1970
Richland, Wa. 99352

10. PROJECT/TASK/WORK UNIT NO.

11. CONTRACT NO.
B5988-7

12. SPONSORING ORGANIZATION NAME AND MAILING ADDRESS (Include Zip Code)
Office of Nuclear Regulatory Research
U.S. Nuclear Regulatory Commission
Washington, DC 20555

13. TYPE OF REPORT
Quarterly Progress Report

PERIOD COVERED (Inclusive dates)
January - March 1980

15. SUPPLEMENTARY NOTES

14. (Leave blank)

16. ABSTRACT (200 words or less)

This report describes progress made in the Light Water Reactor Pressure Vessel Irradiation Surveillance Dosimetry Program during the reporting period.

The primary objective of the multi-laboratory program is to prepare an updated and improved set of dosimetry, damage correlation, and associated reactor analysis ASTM Standards for LWR-PV irradiation surveillance programs. Supporting this objective are a series of analytical and experimental validation and calibration studies in "Standard, Reference, and Controlled Environment Benchmark Fields", reactor "Test Regions", and operating power reactor "Surveillance Positions".

17. KEY WORDS AND DOCUMENT ANALYSIS

17a. DESCRIPTORS

17b. IDENTIFIERS/OPEN-ENDED TERMS

18. AVAILABILITY STATEMENT
Unlimited

19. SECURITY CLASS (This report)
Unclassified

21. NO. OF PAGES

20. SECURITY CLASS (This page)
Unclassified

22. PRICE
$

NRC FORM 335 (7-77)